Sequential actions of phosphatidylinositol phosphates regulate phagosome-lysosome fusion

Andreas Jeschke and Albert Haas*
Cell Biology Institute, University of Bonn, 53121 Bonn, Germany

ABSTRACT Phagosomes mature into phagolysosomes by sequential fusion with early endosomes, late endosomes, and lysosomes. Phagosome-with-lysosome fusion (PLF) results in the delivery of lysosomal hydrolases into phagosomes and in digestion of the cargo. The machinery that drives PLF has been little investigated. Using a cell-free system, we recently identified the phosphoinositide lipids (PIPs) phosphatidylinositol 3-phosphate (PI(3)P) and phosphatidylinositol 4-phosphate (PI(4)P) as regulators of PLF. We now report the identification and the PIP requirements of four distinct subreactions of PLF. Our data show that (i) PI(3)P and PI(4)P are dispensable for the disassembly and activation of (phago)lysosomal soluble *N*-ethylmaleimide-sensitive factor attachment protein receptors, that (ii) PI(3)P is required only after the tethering step, and that (iii) PI(4)P is required during and after tethering. Moreover, our data indicate that PI(4)P is needed to anchor Arl8 (Arf-like GTPase 8) and its effector homotypic fusion/vacuole protein sorting complex (HOPS) to (phago)lysosome membranes, whereas PI(3)P is required for membrane association of HOPS only. Our study provides a first link between PIPs and established regulators of membrane fusion in late endocytic trafficking.

INTRODUCTION

During phagocytosis, professional phagocytes such as macrophages ingest large particles into plasma membrane-derived phagosomes. Phagosomes eventually mature into phagolysosomes

by sequential fusion with early endosomes, late endosomes, and lysosomes (Desjardins *et al.*, 1994). Once phagosomes have fused with lysosomes, the ingested cargo is mixed with microbicidal and degradative lysosome contents, killed, and degraded. Using this machinery, professional phagocytes ingest and dispose of microbes, apoptotic cells, and other particulate matter and contribute to immune defense and tissue remodeling (Flannagan *et al.*, 2012).

As with other membrane fusion events within the endocytic and secretory pathways, fusion of phagosomes with endosomes or lysosomes depends on soluble *N*-ethylmaleimide–sensitive fusion factor attachment protein receptor (SNARE) proteins (Collins *et al.*, 2002; Becken *et al.*, 2010). SNARE-mediated membrane fusion consists of a common sequence of interdependent subreactions, that is, *cis*-SNARE complex disassembly, tethering, docking, and fusion, all of which are regulated by members of conserved protein families, including SNARE proteins, Sec1/Munc18-like (SM) proteins and Ras-like protein from rat brain (Rab) GTPases (Wickner and Rizo, 2017). During tethering, "tethering factors" link Rab GTPases anchored in adjacent membranes and provide an initial, reversible interaction of the membranes to be fused. After tethering, three Q-SNARE helices from one membrane and one R-SNARE helix from the other form a *trans*-SNARE complex (Fasshauer *et al.*, 1998) in a process that can be supported by tethering factors and/or SM proteins (Südhof and Rothman, 2009; Hong and Lev, 2014). The resulting *trans*-SNARE complex pulls the membranes into close apposition (docking). Forces generated by the SNARE pairing

(Weber *et al.*, 1998) and insertion of hydrophobic wedge domains of proteins that are recruited to *trans*-SNARE complexes (e.g., α-SNAP, synaptotagmin 1) eventually lead to lipid bilayer fusion (Wickner and Rizo, 2017). After fusion, the SNARE proteins reside in a *cis*-SNARE complex in the fusion product membrane. To drive a new round of fusion, *cis*-SNARE complexes need to be disassembled in a "priming" reaction (Ungermann *et al.*, 1998), which requires cooperative, ATP-dependent action of the SNARE chaperone *N*-ethylmaleimide–sensitive factor (NSF) and its cochaperone α-soluble NSF attachment protein (α-SNAP; Zhao *et al.*, 2015).

Recent years have identified PIPs as common regulators of SNARE-mediated membrane fusion events (Poccia and Larijani, 2009). PIPs are mono-, bis- or tris-phosphorylated derivatives of the glycerophospholipid phosphatidylinositol (PI) and are generated by phosphorylation of the D3-, D4-, and/or D5-hydroxyl groups of the inositol moiety of PI (Sasaki *et al.*, 2007). PIPs can be interconverted by PIP phosphatases and kinases and are asymmetrically distributed in different subcellular membranes (De Matteis and Godi, 2004; Sasaki *et al.*, 2009). Most often, PIPs recruit and/or allosterically activate "PIP effector" proteins that mediate the PIPs' downstream functions (Rusten and Stenmark, 2006). PIP effectors bind to a single PIP or multiple PIPs through PIP-binding domains (Kutateladze, 2010) and sometimes require additional determinants such as small GTPases or presence of a certain membrane curvature to bind to membranes. This phenomenon is commonly referred to as "coincidence detection" (Carlton and Cullen, 2005). Various fusion regulators, including tethering factors (Simonsen *et al.*, 1998; Christoforidis *et al.*, 1999), SNARE (Cheever *et al.*, 2001; Dai *et al.*, 2007), and SM proteins (Stroupe *et al.*, 2006; Shin *et al.*, 2010) are PIP effectors, indicating that PIPs can organize fusion-relevant factors within membrane microdomains at future fusion sites (Wickner and Rizo, 2017).

Some so-called intracellular pathogens, such as *Mycobacterium tuberculosis* or *Salmonella enterica*, manipulate the PIP composition of the phagosomes in which they reside and they are not delivered to and killed within phagolysosomes, pointing at a role of PIPs in phagolysosome formation (Vergne *et al.*, 2005; Bakowski *et al.*, 2010). However, little is known about how PIPs regulate fusion of phagosomes with endosomes and, especially, with lysosomes. Recently, PI(3)P and PI(4)P have been implicated in phagosome-with-lysosome fusion (PLF) (Jeschke *et al.*, 2015; Levin *et al.*, 2017). These PIP requirements of PLF are reflected in the fact that cell-free content mixing between phagosomes and lysosomes is blocked by the PI(3)P-binding 2xFYVE domain from mouse hepatocyte growth factor-regulated tyrosine kinase substrate (Hrs) (Gillooly *et al.*, 2000) and by the PI(4)P-binding C-terminal P4C fragment of the *Legionella pneumophila* protein SidC (Ragaz *et al.*, 2008; Jeschke *et al.*, 2015).

Subcellular reconstitution techniques to analyze the roles of PIPs in intracellular trafficking have clearly not been sufficiently exploited. This is surprising because a biochemically reconstituted system allows the fast addition and removal from the ongoing reaction of proteins, antibodies, and of membrane-impermeable pharmacologicals; it allows the mixing of components from genetically manipulated cells and kinetic dissection of the actions of inhibitors. Evidently, many mechanistically revealing experiments that can be done using such in vitro systems cannot be done in a living, intact cell. However, only few studies have reconstituted fusion of phagosomes with endosomes (Mayorga *et al.*, 1991; Alvarez-Dominguez *et al.*, 1996; Mukherjee *et al.*, 2000; Vergne *et al.*, 2005) and lysosomes (Jahraus *et al.*, 1998; Peyron *et al.*, 2001; Becken *et al.*, 2010). Moreover, none of these studies has analyzed fusion subreactions so that the order of events that underlie PLF are largely unexplored. Here we have applied cell-free assays to dissect PLF into its subreactions and

to test which of these subreactions depended on PI(3)P and/or PI(4)P. We have developed a toolbox that, together with in cellulo techniques, can analyze the machinery that drives PLF.

RESULTS
We have recently reconstituted the overall reaction of PLF in a cell-free assay. To this end, purified phagosomes and lysosomes were incubated under "fusion assay conditions," that is, at a physiological temperature and in the presence of ATP and soluble cytosolic factors. Transfer during fusion of a fluorescent, luminal tracer from lysosomes into phagosomes, quantified by fluorescence microscopy, serves as a measure of content mixing between these compartments (Becken *et al.*, 2010; Jeschke *et al.*, 2015). Since content mixing is the last step of membrane fusion, inhibition of any preceding fusion subreaction decreases the extent of content mixing. For reasons of clarity, "PLF" will denote the complete sequence of subreactions leading to phagosome-with-lysosome fusion.

### SNARE priming requires neither PI(3)P nor PI(4)P
During "priming," ATP-loaded NSF is recruited to *cis*-SNARE complexes by α-SNAP. NSF hydrolyzes ATP, *cis*-SNARE complexes become disassembled, and α-SNAP is released into the cytosol. When priming is inhibited in homotypic early endosome (Colombo *et al.*, 1998) or yeast vacuole fusion (Mayer *et al.*, 1996), α-SNAP remains membrane-associated. Here we show that incubation of phagosomes and lysosomes in the absence of ATP increased steady-state levels of α-SNAP on (phago)lysosome membranes, as did preincubation of the compartments with fusion-blocking concentrations of NSF-inhibiting *N*-ethylmaleimide (NEM) (Figure 1, A and B). As expected, NEM that had been inactivated by equimolar concentrations of dithiothreitol (DTT) did not cause accumulation of α-SNAP on (phago)lysosome membranes (Figure 1, A and B).

To test whether PI(3)P and/or PI(4)P were required for priming, we incubated phagosomes and lysosomes under fusion assay conditions in the presence of 10 μM of PI(3)P-binding 2xFYVE domain, PI(4)P-binding P4C, or the purification tag GST or in the absence of ATP. We then determined the amount of α-SNAP on (phago)lysosome membranes by immunoblotting. Whereas omission of ATP from the reaction mixture led to α-SNAP accumulation on (phago)lysosomes (Figure 1, C and D), neither addition of GST, nor of PIP-binding domains affected steady-state binding levels of α-SNAP. Apparently, PI(3)P and PI(4)P were dispensable for the priming subreaction of PLF (Figure 1, C and D).

Phagosome-to-lysosome binding depends on PI(4)P but not PI(3)P
To test whether PI(3)P and/or PI(4)P were required for phagosome-to-lysosome binding, we designed an in vitro reaction that measures attachment of phagosomes to lysosomes rather than their fusion. The binding step of membrane fusion is transient, that is, the proportion of attached compartments initially increases and then declines as the compartments proceed to fusion (Hernandez *et al.*, 2012).

To block PLF after phagosome-to-lysosome binding and to facilitate the analysis of attachment (Mayer and Wickner, 1997), we used lysophosphatidylcholine C12 (LPC-12), a late-stage inhibitor of membrane fusion. LPC-12 is an inverted cone-shaped lipid whose integration into the outer leaflet of a membrane bilayer induces positive curvature and inhibits the lipid mixing step of membrane fusion (Melia *et al.*, 2006). As expected, LPC-12 dose-dependently blocked PLF (Figure 2C) without affecting the priming subreaction (Supplemental Figure S3; Reese and Mayer, 2005). Notably, in
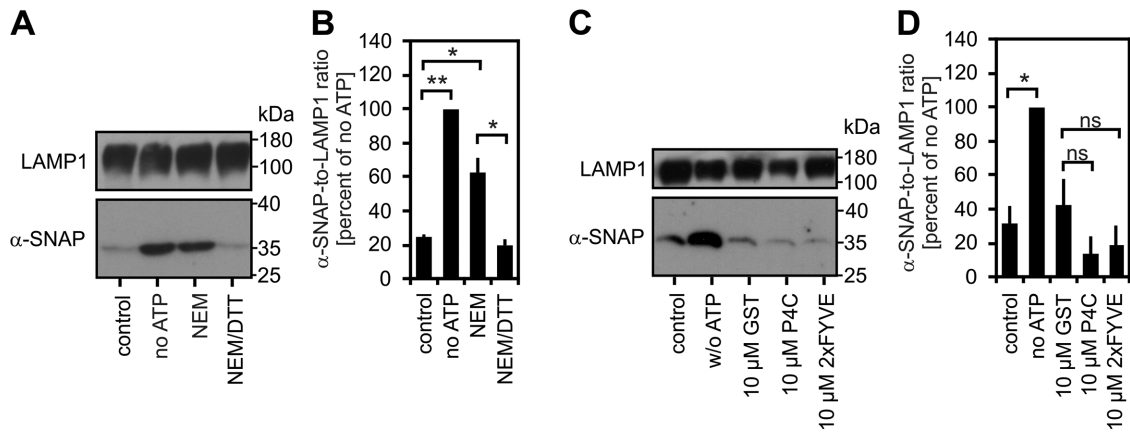
FIGURE 1: Uncomplexed PI(3)P and PI(4)P are not needed for α-SNAP release during the PLF reactions. (A) Phagosomes and lysosomes were incubated under fusion assay conditions (60 min, 37°C) in the presence ("control") or absence of ATP ("no ATP") or in the presence of ATP and after preincubation with 2 mM NEM ("NEM") or with 2 mM NEM inactivated with equimolar concentrations of DTT (15 min on ice) ("NEM/DTT"). Compartments were sedimented (16,100 × g, 4°C, 10 min) and analyzed for α-SNAP by immunoblotting. LAMP1 staining was used as a control for equal protein load. (C) Steady-state levels of α-SNAP on phagosome and lysosome membranes were assayed as in A after incubation of the compartments with ATP and 10 μM of GST, 2xFYVE, or P4C or without ATP. (B, D) Densitometric quantification of immunoblots as in A or C from three independent experiments (n = 3). Steady-state levels of α-SNAP are expressed as a α-SNAP-to-LAMP1 ratio. This ratio was set as a 100% for "no ATP" samples in each experiment. Bars represent means ± SEM. *p < 0.05, **p < 0.01 for two-tailed unpaired Student's t test. ns: not significant, p > 0.05.

samples that received more than 50 μM LPC-12, unfused phagosomes were often bound to lysosomes (Figure 2, A vs. B), indicating that LPC-12 blocked PLF without affecting phagosome-to-lysosome binding. LPC-12 did not damage (phago)lysosome membranes even at 100 μM, as shown by retention of the fluid phase tracer bovine serum albumin (BSA)-rhodamine-biotin (BSA-rho-bio) at all times (Supplemental Figure S1). To routinely quantify binding, phagosomes and lysosomes were incubated under fusion assay conditions in the presence of 100 μM LPC-12, and phagosomes were reisolated by floatation in a density gradient and analyzed for bound lysosomes by fluorescence microscopy.

In uninhibited control samples, routinely approximately 40% of all phagosomes were associated with lysosomes. This was often ~3 times the percentage of phagosomes fusing (colocalizing with lysosomal BSA-rho-bio) in parallel samples (Figure 2D, "60-min" samples, binding vs. fusion). A similar ratio between docking and fusion efficiencies has been reported earlier for cell-free homotypic early endosome fusion (Geumann et al., 2008).
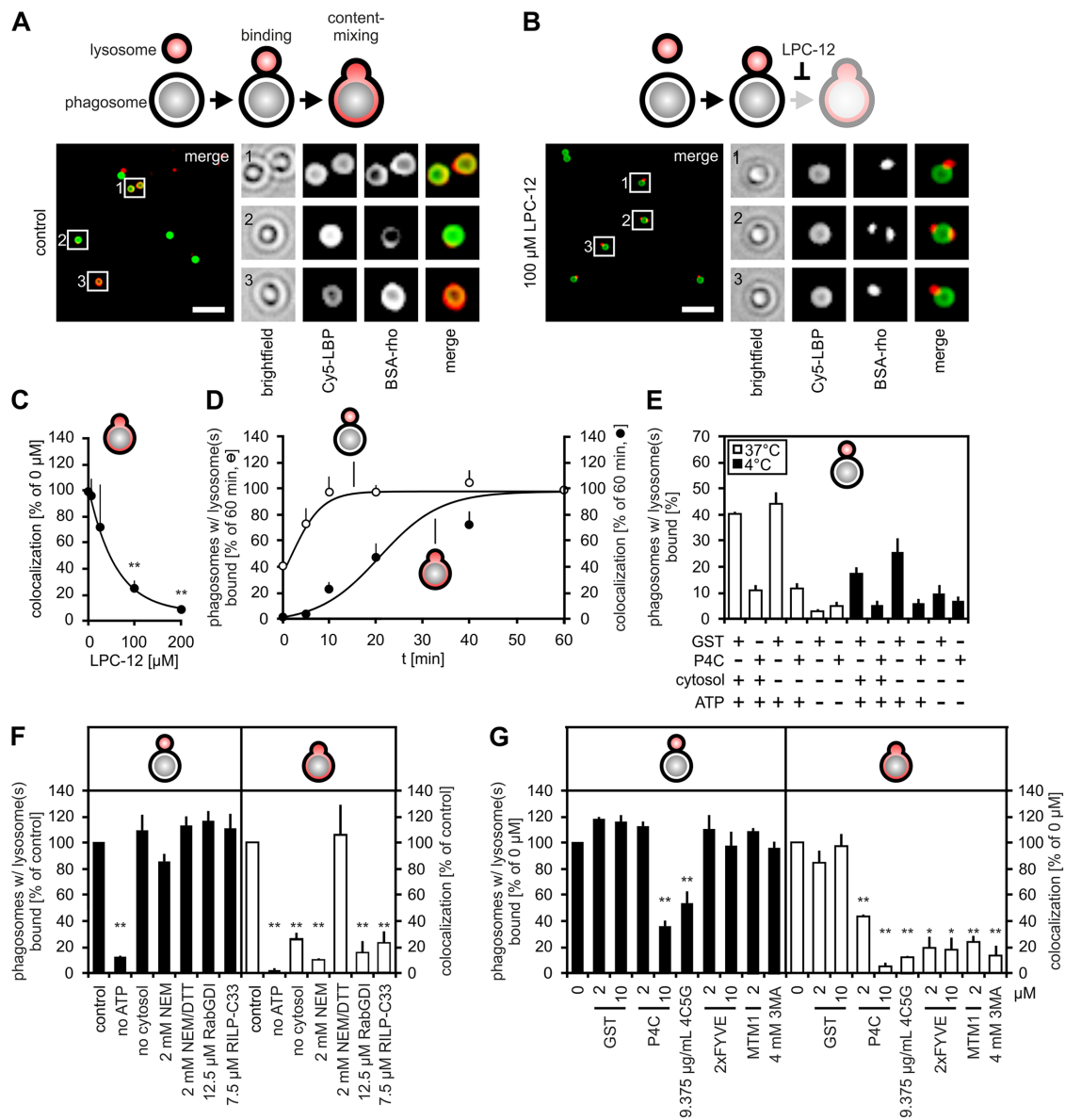
Phagosome-to-lysosome binding required ATP (Figure 2F) and proceeded quickly, reaching maximum values at ~5–10 min (Figure 2D), whereas content mixing assayed in parallel samples was completed at approximately 40 min (Figure 2D). Samples incubated on ice for 60 min ("0-min" samples) displayed approximately 40% of the maximum binding activity (Figure 2D) that was strictly ATP dependent (Figure 2E), suggesting that it represents authentic tethering/docking.

Unlike PLF, phagosome-to-lysosome binding did not require addition of cytosol (Figure 2F), suggesting that all proteins that were needed for attachment were copurified with the compartments. NEM, which completely blocked SNARE priming (Figure 1, A and B) and fusion (Figure 2F, white bars) did not interfere with phagosome-to-lysosome binding (Figure 2F, black bars). This indicated that priming was not a prerequisite for attachment, which is also true for homotypic early endosome fusion (Christoforidis et al., 1999; Geumann et al., 2008). By contrast, vacuole-to-vacuole binding

during homotypic yeast vacuole fusion requires completion of priming (Mayer and Wickner, 1997).

Given the well-established role of Rab GTPases in tethering (Grosshans et al., 2006), it was surprising that RabGDI, which extracts GDP-bound Rab proteins from membranes, blocked content mixing but did not interfere with phagosome-lysosome binding (Figure 2F). Moreover, RabGDI did not block release of α-SNAP from (phago)lysosome membranes (Supplemental Figure S3), suggesting that it targets fusion subreactions other than priming and attachment. Like RabGDI, RILP-C33 (a C-terminal fragment of RILP, Rab-interacting lysosomal protein) which binds to GTP-complexed Rab7 (Cantalupo et al., 2001) and Rab34 (Colucci et al., 2005) and which competitively blocks PLF in intact cells (Harrison et al., 2003) inhibited content mixing but not phagosome-to-lysosome binding.

To test whether PI(3)P and/or PI(4)P are required for phagosome-to-lysosome binding, we assayed binding and content mixing in parallel samples that received 2 or 10 μM of 2xFYVE domain, P4C, or GST. 2xFYVE did not affect phagosome-to-lysosome binding but strongly reduced content mixing at 2 and 10 μM (Figure 2G). Likewise, dephosphorylation of PI(3)P by myotubularin 1 (MTM1) or blocking the generation of this PIP by the phosphatidylinositol-3-kinase (PI3K) inhibitor 3-methyladenine (3-MA) inhibited the overall process of PLF but not phagosome-to-lysosome binding (Figure 2G). PI(4)P-sequestering P4C, by contrast, blocked binding and content mixing. Notably, phagosome-to-lysosome binding was less sensitive toward P4C than was content mixing: at 2 μM, P4C blocked content mixing by approximately 60% yet did not inhibit binding at all (Figure 2G). This suggested that the overall process of PLF requires at least a second PI(4)P-dependent step after phagosome-to-lysosome binding. F_{ab} fragments of 4C5G, a monoclonal antibody (mAb) that inhibits class II phosphatidylinositol 4-kinase (PI4K) (Endemann et al., 1991) also blocked binding and content mixing (Figure 2G), validating the involvement of PI4KII-generated PI(4)P in phagosome-to-lysosome binding.

FIGURE 2: Identification of molecular determinants of phagosome-to-lysosome binding. (A, B) Representative fluorescence micrographs from cell-free PLF reactions incubated in the absence (A) or presence (B) of 100 μM LPC-12. Magnified regions are boxed. Cy5-labeled LBPs are displayed in green, lysosomes in red. Bar: 5 μm. Schematic drawing showing subreactions leading to PLF and the site of action of LPC-12. (C) Cell-free PLF in the presence of LPC-12 at the concentrations indicated. (D) Kinetics of phagosome-to-lysosome binding (open circles) and fusion (filled circles) were assayed in parallel samples. At times indicated reactions were set on ice. Binding and colocalization at 60 min were set as 100%, which corresponds to 44.5% (±9.21 [SEM]) and 15.3% (±7.76 [SEM]) of phagosomes bound to lysosome(s) or colocalized with lysosomal BSA-rho-bio (three independent experiments [$n = 3$]). (E) Phagosome-lysosome binding was assayed at either 37°C (white bars) or 4°C (black bars) under conditions specified. (F, G) Phagosomes and lysosomes were incubated for 60 min at 37°C under conditions specified. Binding (black bars) was assayed in the presence of LPC-12, fusion (white bars) was assayed in its absence. All data represent means ± SEM from at least three independent experiments ($n = 3$). *$p < 0.05$, **$p < 0.01$ for two-tailed unpaired Student's t test.

The above experiments analyzed, strictly speaking, membrane fusion between phagolysosomes and lysosomes that occurs during repeated PLF in the cell (Desjardins *et al.*, 1994). We wondered whether the first round of fusion between a "late phagosome" and a lysosome would have the same requirements. Therefore we also analyzed tethering and content mixing between late phagosomes and lysosomes for an involvement of PI(4)P. Both late phagosomes and phagolysosomes required ATP and PI(4)P to bind to and to fuse with lysosomes (Supplemental Figure S2). Therefore, by reconstituting

phagolysosome-lysosome fusion, we also investigate events that occur during preceding fusion between late phagosomes and lysosomes, a step that is central to the maturation process.

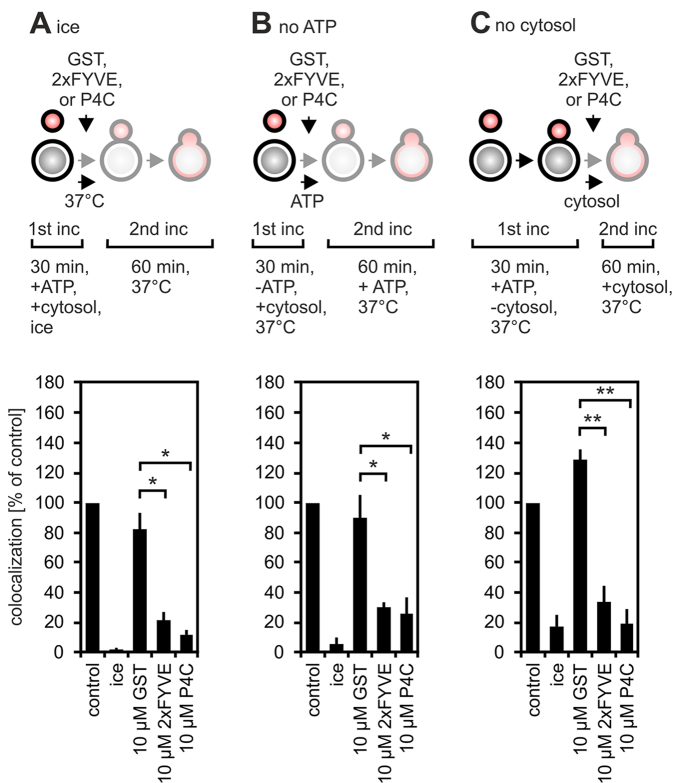## PI(3)P and PI(4)P are required after phagosome-to-lysosome binding

Phagosome-to-lysosome binding required ATP and a physiological temperature but did not depend on cytosol addition (Figure 2, D, "0-min" samples, and F). Building on this observation, we blocked

the fusion sequence at different stages. We arrested the process before binding by incubation on ice or at 37°C in the absence of ATP, or we arrested the reaction after binding by incubating at 37°C without cytosol. At 30 min of incubation under the conditions specified above, "no ATP" and "no cytosol" samples were supplemented with ATP and cytosol, respectively. "Ice" samples received buffer only. Samples received buffer or 10 µM of 2xFYVE, P4C, or GST as indicated and were incubated for an additional 60 min at 37°C or on ice, before fusion was assayed.

Irrespective of the type of preincubation, PLF did not become resistant toward 2xFYVE or P4C (Figure 3). PLF was sensitive toward the PI(3)P-binding 2xFYVE domain and PI(4)P-binding P4C even after removal of a postbinding block in "no cytosol" samples (Figure 3C). This again placed the PI(3)P-requiring step after binding. Moreover, these data indicated that the overall reaction of PLF includes a second PI(4)P-dependent step after phagosome-to-lysosome binding.

The second PI(4)P-dependent step follows the PI(3)P-requiring step

Attachment was sensitive toward PI(4)P-binding P4C, suggesting that PI(4)P is needed for phagosome-to-lysosome binding. To test this hypothesis, we studied the requirements of binding using a different approach.


FIGURE 3: PLF requires PI(3)P and PI(4)P after phagosome-to-lysosome binding. Cell-free fusion reactions of five times the standard volume were incubated for 30 min on ice (A) or at 37°C in the absence of either ATP (B) or cytosol (C). "No ATP" and "no cytosol" samples then received ATP and cytosol, respectively. Aliquots of these reactions were supplemented with buffer or 10 µM of GST, 2xFYVE, or P4C and incubated for an additional 60 min at 37°C or on ice. Colocalization in samples incubated without recombinant proteins during the second incubation was set as 100% ("control"). Data represent means ± SEM from three independent experiments ($n = 3$). *$p < 0.05$, **$p < 0.01$ for two-tailed unpaired Student's t test.

Polyethylene glycol (PEG) dehydrates membranes, which lowers the energy barrier for membrane-to-membrane binding and hemifusion. Owing to this property, PEG has been used to artificially tether liposomes in reconstituted membrane fusion systems (Dennison *et al.*, 2006; Hickey and Wickner, 2010; Furukawa and Mima, 2014). As expected, PEG markedly stimulated the extent of PLF (Figure 4A), yet it only slightly increased the rate of content mixing (Figure 4B). PLF in the presence or absence of PEG was equally sensitive to omission of ATP or cytosol (Figure 4C), authenticating PEG-stimulated PLF as a physiologically relevant process. If PI(4)P was required to connect phagosome and lysosome membranes prior to fusion, then PEG, as an artificial tethering factor, could possibly render PLF resistant to a PI(4)P-binder. Here, P4C did not inhibit phagosome-to-lysosome binding in the presence of 2.5% (wt/vol) PEG (Figure 4D), yet content mixing was equally sensitive to P4C in the presence or absence of PEG (Figure 4E). These data suggest that PEG bypassed the PI(4)P requirement for binding but not for content mixing and that therefore PI(4)P is required before and after attachment.

On the other hand, PEG made PLF less sensitive to the PI(3)P-binding 2xFYVE domain (Figure 4F). This was unexpected since the 2xFYVE domain blocked the overall reaction of PLF after phagosome-to-lysosome binding (Figures 2 and 3), that is, after the step that PEG was expected to bypass. We propose that PEG stimulates PLF subreactions downstream of phagosome-to-lysosome binding. To test this hypothesis, we analyzed whether PEG stimulated PLF even after completion of binding. To this end, we assayed in parallel the kinetics of phagosome-to-lysosome binding, of content mixing, and of stimulation of fusion by addition of PEG. Large-scale fusion and LPC-12-containing binding reactions were incubated for 60 min at 37°C. At different times after the beginning of the incubation, aliquots of these reactions were set on ice to stop binding or fusion and the proportion of phagosomes bound to or fused with lysosomes was quantified. These data indicated the kinetics of binding and fusion reactions. At each time indicated, a second aliquot of the fusion reaction was supplemented with 2.5% (wt/vol) PEG and incubated at 37°C for the remainder of the 60-min incubation period, yielding the information of how long the overall PLF reaction would be stimulable by PEG. PEG strongly stimulated fusion, even if added at 40 min after beginning of the incubation (Figure 4H, red curve). Phagosome-to-lysosome binding, however, reached maximum values by 10 min (Figure 4H). This suggested that PEG stimulated an additional, later, step of PLF. As addition of PEG rendered PLF less sensitive toward the lipid-mixing inhibitor LPC-12 (Figure 4G), lipid mixing between phagosomes and lysosomes is the prime candidate for a second PEG target.

Notably, addition of PEG enabled fusion in reactions that had been arrested at the PI(3)P-dependent step by preincubation in the presence of 2xFYVE domain (Figure 5A). This fact was used to test whether the second PI(4)P-dependent step lies after of the 2xFYVE fusion block. To this end, fusion reactions were kept on ice ("ice" samples) or at 37°C with 2 µM 2xFYVE domain ("2xFYVE" samples). Both conditions largely blocked fusion. After 30 min, aliquots of these reactions were supplemented with 2.5% (wt/vol) PEG and buffer and incubated for an additional 60 min on ice or at 37°C. Incubation on ice completely blocks fusion, even in the presence of PEG (Figure 4, A and B, "0 min" samples). Hence, samples kept on ice during the second incubation reveal how much fusion has occurred during the preincubations. "Control" samples, incubated at 37°C during the second incubation, in turn, reveal how much fusion has occurred during the second incubation. In 2xFYVE-pretreated reactions, incubation in the
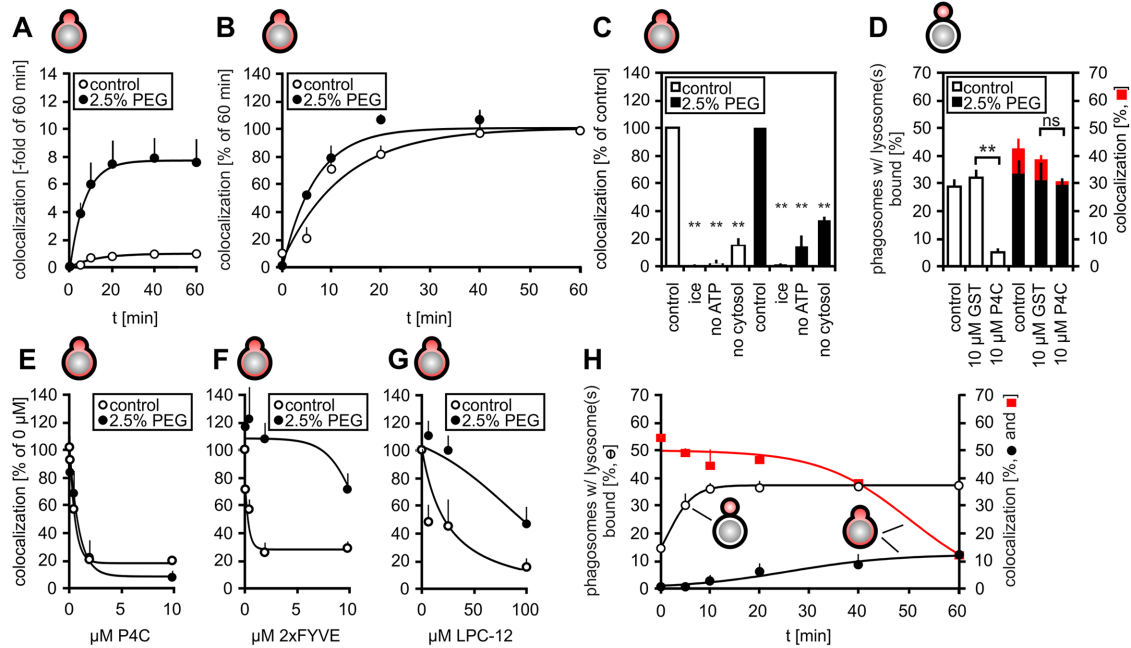
FIGURE 4: Identification of a second PI(4)P-dependent step after phagosome-to-lysosome binding. (A, B) Cell-free PLF reactions were incubated in the presence or absence of 2.5% (wt/vol) PEG at 37°C for various times. (A) Fold values are normalized to colocalization in "60-min" samples incubated without PEG. (B) To directly compare the rates of fusion, colocalization of phagosomes with lysosome contents in "60-min" samples was set as 100% for both conditions (± PEG). (C) Cell-free PLF reactions were incubated in the absence or presence of 2.5% (wt/vol) PEG for 60 min at 37°C under conditions specified. Colocalization in control samples was set as 100%. (D) Phagosome-to-lysosome binding assayed in samples incubated with cytosol and ATP for 60 min at 37°C with 200 μM LPC-12 and in the presence (black bars) or absence (white bars) of 2.5% (wt/vol) PEG. In the presence of PEG, some phagosomes and lysosomes overcame the fusion block by LPC-12. Given that these compartment pairs must have bound to each other before they fused, the extent of fusion (red bars) was added to the extent of binding in PEG-containing samples. PLF was completely inhibited in samples incubated without PEG as indicated by the lack of red bars. (E–G) Cell-free PLF reactions were run in the presence (filled circles) or absence of 2.5% (wt/vol) PEG (open circles) and P4C, 2xFYVE, or LPC-12 at various concentrations. Colocalization in "0 μM" samples was set as 100%. (H) The kinetics of phagosome-to-lysosome binding (open circles) and fusion (filled circles) were assayed in parallel samples. Another set of PLF reactions received 2.5% (wt/vol) PEG at times indicated (red curve). In these samples, PLF was assayed after a total of 60 min incubation at 37°C. All data represent means ± SEM from three independent experiments ($n = 3$). For C and D: *$p < 0.05$, **$p < 0.01$ for two-tailed unpaired Student's t test. ns: not significant, $p > 0.05$.

presence of PEG for an additional 60 min at 37°C ("control") led to a comparable extent of fusion as observed in reactions preincubated on ice. This suggested that PEG could overcome fusion inhibition by 2xFYVE, not only when added simultaneously with the PIP-binder (Figure 4F) but also when added afterward (Figure 5A). Addition of P4C during the second incubation strongly inhibited fusion in ice- and 2xFYVE-preincubated samples (Figure 5A), indicating that there is a second PI(4)P-dependent step after the PI(3)P requirement.

To validate this hypothesis, we assayed the kinetics of fusion inhibition by 2xFYVE or P4C: A large-scale PLF reaction was incubated for 60 min at a decreased temperature of 27°C to slow the subreactions and to allow a temporal dissection of the events. At the times indicated, aliquots were withdrawn and either set on ice to reveal the kinetics of the fusion reaction ("ice" samples) or supplemented with 10 μM 2xFYVE or 10 μM P4C and incubated at 27°C for the remainder of the incubation time. Colocalization in 2xFYVE- or P4C-containing samples indicates when PLF became resistant toward an inhibitor. PLF was resistant to the 2xFYVE domain after ~40 min, whereas it never acquired resistance to P4C (Figure 5B). This is in line with PI(4)P being required after the PI(3)P-dependent step. For interpretation

purposes, it should be noted that this kind of experiment captures only the latest subreaction that is inhibited by a compound.

In sum, P4C blocks two subreactions of PLF, attachment and content mixing, whereas 2xFYVE blocks PLF after the binding reaction yet before the second PI(4)P-dependent step.

PI(3)P and PI(4)P are present on phagosomes and lysosomes bound to each other

Our data suggested that both PI(3)P and PI(4)P are required after phagosome-to-lysosome binding. If this was correct, then these lipids should be present on at least one of the fusion partners when phagosomes and lysosomes were bound to each other. We tested this by incubating phagosomes and lysosomes under fusion assay conditions in the presence of 100 μM LPC-12 and 2 μM of 2xFYVE, P4C, or GST. LPC-12 served to arrest the overall reaction of PLF after the binding stage and to facilitate analysis of tethered/docked phagosomes and lysosomes. PIP binders were added to visualize PI(3)P or PI(4)P on the compartments via anti-GST antibodies. At the concentrations applied, 2xFYVE and P4C did not interfere with phagosome-to-lysosome attachment (Figures 2G and 6C) and hence could be used solely to track PIPs.
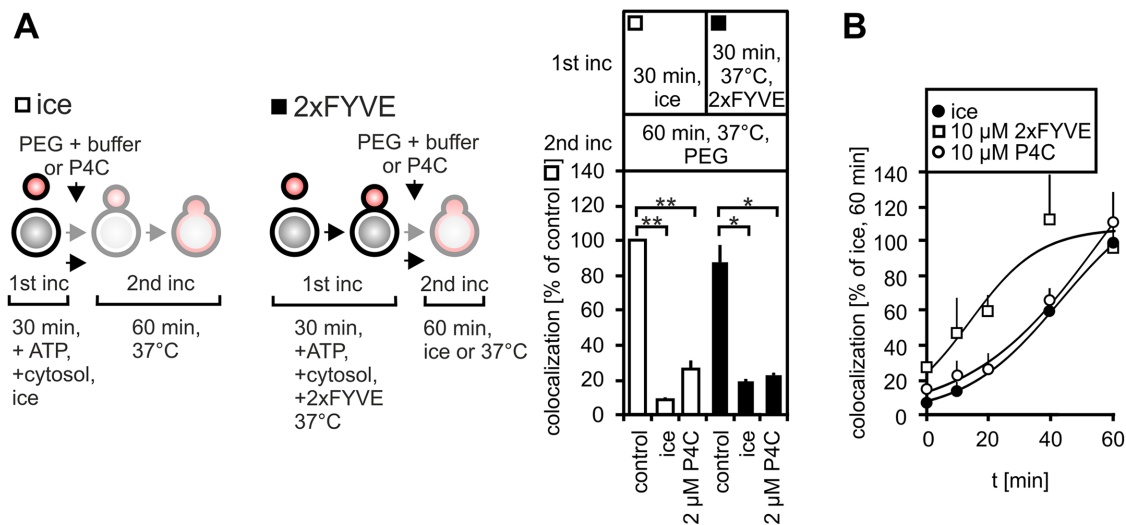
FIGURE 5: The second PI(4)P-dependent step follows the PI(3)P requirement. (A) Cell-free PLF reactions were incubated on ice or with 2 μM 2xFYVE at 37°C for 30 min ("1st incubation"). Reactions then received 2.5% (wt/vol) PEG. Aliquots of these reactions were supplemented with buffer or 2 μM P4C and incubated for an additional 60 min at 37°C or on ice ("2nd incubation"). Data represent means ± SEM from three independent experiments ($n = 3$). *$p < 0.05$, **$p < 0.01$ for two-tailed unpaired Student's t test. (B) A large-scale PLF reaction was incubated at 37°C. Aliquots were withdrawn at the times indicated and set on ice. Additional aliquots were supplemented with 10 μM of 2xFYVE or P4C and incubated at 37°C until a total of 60 min incubation was completed. Data represent means ± SEM from five independent experiments ($n = 5$).

The reaction products were categorized depending on attachment status and lipid possession. As depicted in Figure 6, A and B, phagosomes had either not bound to a lysosome and they contained the respective lipid (condition 2) or not (condition 1), or they had bound to a lysosome, and the lipid was present only in the phagosome (condition 6), only in the lysosome (condition 5), in both (condition 4), or in neither of the compartments (condition 3). Notably, PI(3)P or PI(4)P was present on either or on both compartments in more than 80% of phagosomes and lysosomes bound to each other (Figure 6C, conditions 4+5+6 divided by conditions 3+4+5+6). This observation well agrees with roles of PI(3)P and PI(4)P in late, post-binding steps of PLF. Most often, the lipids were present in both of the attached compartments (Figure 6C, condition 4). Given that not all phagosome-lysosome pairs proceed to fusion (Figure 4H, "60-min" samples fusion vs. binding), this supports the view that PLF requires presence of PI(3)P and PI(4)P on both compartments.

The roles of PI(3)P and PI(4)P in PLF are linked to the HOPS complex

PIPs often exert their functions by anchoring PIP effector proteins to membranes. The homotypic fusion/vacuole protein sorting complex (HOPS) complex is a six-subunit tethering complex conserved from yeast to mammals. Comprehensive studies of homotypic yeast vacuole fusion revealed that yeast HOPS mediates tethering (Hickey and Wickner, 2010) and *trans*-SNARE complex assembly (Baker *et al.*, 2015) and that it binds to PIPs including PI(3)P and PI(4)P (Stroupe *et al.*, 2006). Together with the fact that mammalian HOPS is required for late endosome-lysosome fusion (Pols *et al.*, 2013), HOPS was a good candidate effector protein for PI(3)P and/or PI(4)P in PLF. To address this issue, we assayed phagosome-to-lysosome binding, PLF, and steady-state levels of the HOPS complex subunit Vps41 on phagosomes and lysosomes in vitro in the presence or absence of PI(3)P-binding 2xFYVE domain, PI(4)P-binding P4C, or GST or in the absence of ATP (Figure 7). Since

mammalian HOPS is recruited to late endocytic compartments by binding to Arl8b (Arf-like GTPase 8b; Khatter *et al.*, 2015) and/or by binding to the Rab7 effector RILP (van der Kant *et al.*, 2013; Lin *et al.*, 2014), we also analyzed the impact of PIP-binding domains on steady-state levels of (phago)lysosomal Arl8 and Rab7. Phagosome-to-lysosome binding and PLF assayed in parallel samples (Figure 7B) yielded similar results as before (Figure 2).

Incubation in the absence of ATP decreased concentrations of bound Arl8, whereas it did not affect levels of Rab7 and Vps41 (Figure 7B). Sequestration of PI(3)P decreased steady-state levels of Vps41 on (phago)lysosomes, but it did not impact on the amounts of Arl8 or of Rab7 (Figure 7B). Sequestration of PI(4)P, on the other hand, decreased Arl8 and Vps41 levels (Figure 7B). None of the conditions tested reduced steady-state levels of Rab7 on (phago)-lysosome membranes (Figure 7B). Moreover, addition of GST did not affect steady-state levels of Vps41, Rab7, or Arl8 as compared with "control" samples.

2xFYVE and P4C decreased Vps41 levels on (phago)lysosomes or levels of both Arl8 and Vps41 also when cytosol was omitted from the incubations (Figure S4). This suggested that the PIP binders not only blocked the recruitment of Arl8 and/or Vps41 from the cytosol but also removed already-bound Arl8 and Vps41 from the membranes and that they therefore are needed to anchor these proteins on (phago)lysosomes.

Interestingly, membrane association of HOPS and phagosome-to-lysosome binding were uncoupled. Accordingly, phagosome-to-lysosome binding was normal in samples containing 2xFYVE, although levels of the HOPS subunit Vps41 were decreased (Figure 7B, "2xFYVE" samples). Moreover, when ATP was omitted from the incubations, phagosomes did not bind to lysosomes even though levels of Vps41 remained high (Figure 7B, "no ATP" samples).

In contrast to the situation with Vps41, reduced Arl8 concentrations correlated with decreased phagosome-to-lysosome binding (Figure 7B, "no ATP" and "P4C" samples).
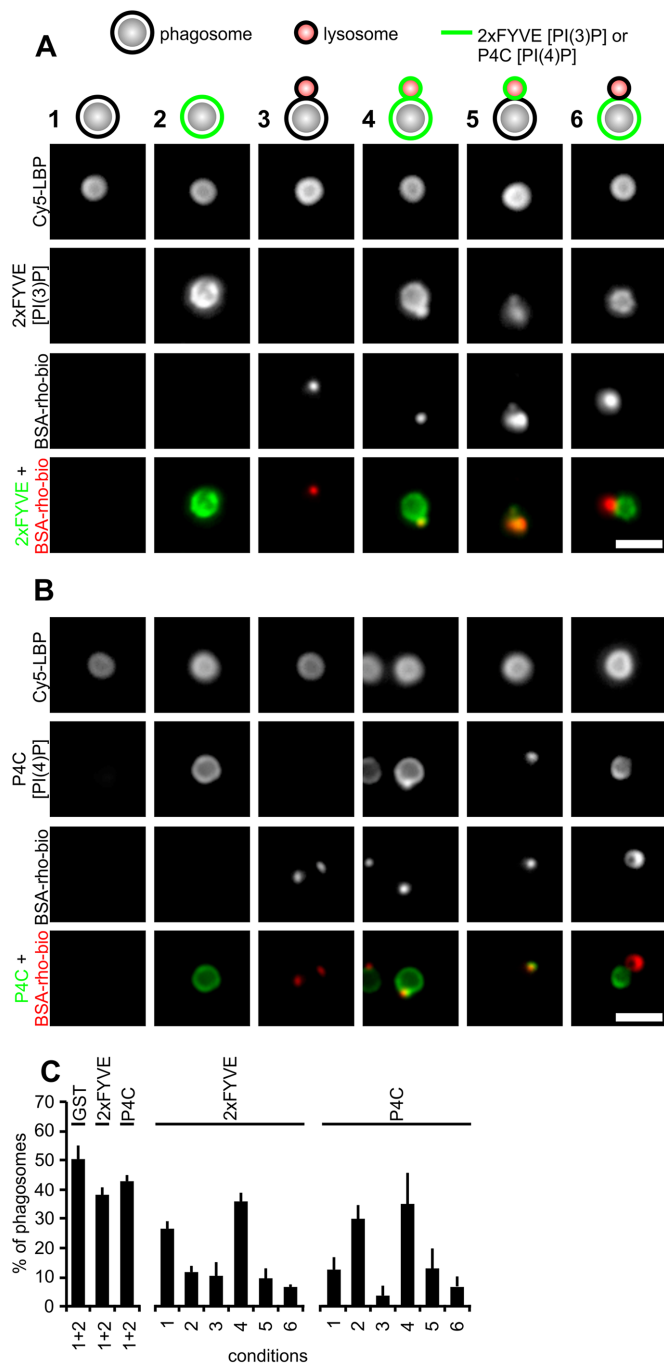
FIGURE 6: Phagosomes and lysosomes that are bound to each other contain PI(3)P and/or PI(4)P. Phagosomes and lysosomes were incubated for 60 min at 37°C with ATP and cytosol and in the presence of 100 µM LPC-12 plus 2 µM of GST, P4C, or 2xFYVE. Phagosomes and bound lysosomes from reaction mixtures were floated in density gradient centrifugation and stained for associated GST, P4C, or 2xFYVE. Phagosomes were then categorized according to the following phenotypes: Phagosomes are not bound to a lysosome and contain the respective lipid (condition 2) or not (condition 1). Phagosomes are bound to a lysosome and the lipid is present in neither of the compartments (condition 3). Phagosomes are bound to a lysosome and the lipid is present in the phagosome (condition 6), in the lysosome (condition 5), or in both of the compartments (condition 4). (A, B) Representative micrographs for each of the above phenotypes for 2xFYVE (A) or P4C (B). Scale bar: 2 µm. (C) Quantification of the various phenotypes as indicated. At least

DISCUSSION

Using a cell-free assay of fusion between phagosomes and lysosomes, we provide evidence that PLF comprises at least four biochemically distinct steps, that is, 1) a *cis*-SNARE complex disassembly step, 2) a phagosome-to-lysosome binding step, 3) an early postbinding step, and 4) a late postbinding and/or content mixing step. Moreover, we have assigned PI(3)P and PI(4)P to these steps: PI(3)P is required only for an early postbinding step, whereas PI(4)P is needed for phagosome-to-lysosome binding and for a late postbinding step.

The priming step of PLF
The priming step of PLF depended on ATP and on NSF activity but it was not inhibited by RabGDI or the lipid-mixing inhibitor LPC-12, similarly as reported for homotypic fusion between yeast vacuoles (Mayer *et al.*, 1996; Reese and Mayer, 2005) or between early endosomes (Colombo *et al.*, 1998). Little is known about the PIP requirements of SNARE complex disassembly: as yet, a single report identified a PIP, that is, phosphatidylinositol 4,5-bisphosphate (PI(4,5)P$_2$), as required for priming of yeast vacuolar SNAREs (Mayer *et al.*, 2000). However, it remained unclear how it affected Sec18p (yeast NSF) and Sec17p (yeast α-SNAP) function.

We observed here that priming of (phago)lysosomal SNAREs was resistant to fusion-inhibiting concentrations of PI(3)P- or PI(4)P-binding protein domains, suggesting that sequestration of the corresponding lipids blocks PLF by inhibition of subreactions other than priming.

Inhibition of priming did not block phagosome-to-lysosome binding, suggesting that binding occurs before or independently of priming. This is similar to tethering/docking of early endosomes, which occurs normally when priming is inhibited (Christoforidis *et al.*, 1999; Geumann *et al.*, 2008). Since priming is a prerequisite for *trans*-SNARE complex assembly, phagosome-to-lysosome binding did not depend on SNARE pairing and hence represents tethering rather than docking. Similarly, clustering of yeast vacuoles or of early endosomes is sensitive to inhibitors of tethering but not to inhibitors of SNARE pairing (Wang *et al.*, 2003; Geumann *et al.*, 2008).

The tethering step of PLF
Delivery of endocytosed material from late endosomes to lysosomes requires a complex interplay of several protein factors, including Arl8, Rab7, RILP, Pleckstrin homology and RUN domain containing M1 (PLEKHM1), and the HOPS complex (Marwaha *et al.*, 2017). Based on observations on homotypic yeast vacuole fusion, mammalian HOPS was assumed to act as a tether linking late endocytic compartments prior to fusion. HOPS interacts with Arl8b (Khatter *et al.*, 2015) and indirectly binds to Rab7 via RILP (van der Kant *et al.*, 2013). PLEKHM1 also binds to HOPS and could act as a tether by itself, as it possesses independent binding sites for both Arl8 and Rab7 (Marwaha *et al.*, 2017). Of these proteins, Arl8 (Garg *et al.*, 2011), Rab7, RILP (Harrison *et al.*, 2003), and HOPS (Kinchen *et al.*, 2008) have been implicated in PLF.

However, RabGDI, which extracts Rab(GDP) proteins from membranes (Ullrich *et al.*, 1993) and which removes Rab7 from purified lysosomes (Mullock *et al.*, 1998), inhibited the overall process of PLF but did not affect phagosome-to-lysosome binding. Likewise, the

---

50 phagosomes were analyzed for association of lysosomes and colocalization with 2xFYVE or P4C. Data are means ± SEM from three independent experiments (*n* = 3).
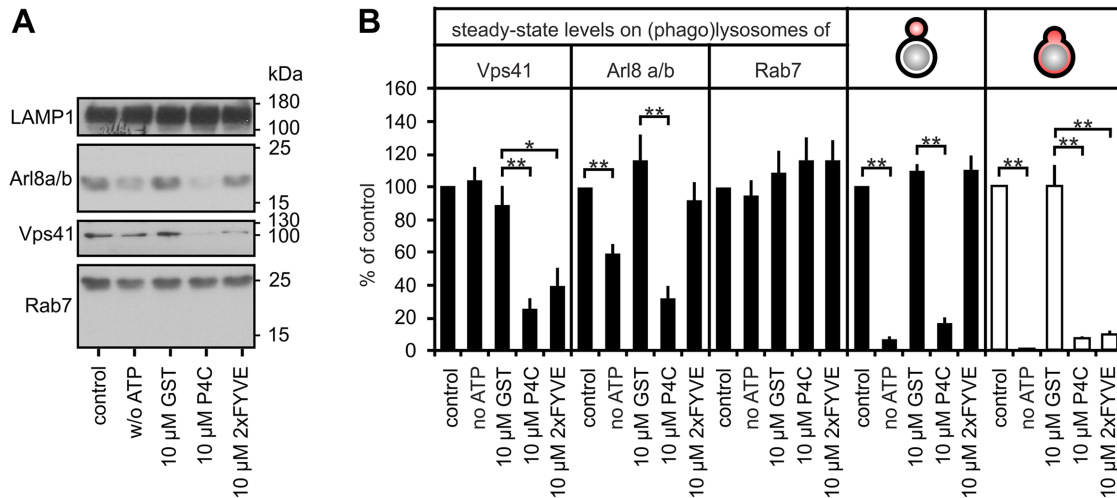
FIGURE 7: Sequestration of PI(3)P or PI(4)P releases Vps41 and/or Arl8a/b from (phago)lysosome membranes. PLF reactions of thrice the standard volume and LPC-12-containing binding reactions were incubated in the presence of ATP and recombinant proteins indicated or without ATP for 60 min at 37°C. LPC-12-containing samples were used to assay binding (B, black bars, binding symbol). One volume of the fusion reactions was used to assay PLF (B, white bars, fusion symbol). The remaining two volumes were centrifuged (16,100 × g, 4°C, 30 min). Sedimented compartments were resuspended in SDS sample buffer and analyzed for proteins indicated by SDS–PAGE and immunoblotting. (A) Representative immunoblots. (B) Quantification of immunoblots as in A and of phagosome-to-lysosome binding and content mixing in six independent experiments ($n = 6$). Error bars represent SEM. *$p < 0.05$, **$p < 0.01$ for two-tailed unpaired Student's t test.

Rab7(GTP)-binding domain of RILP, RILP-C33 (Cantalupo *et al.*, 2001), which blocks PLF in intact cells (Harrison *et al.*, 2003), did not block attachment but PLF in vitro. This implies that Rab GTPases, especially Rab7, are not needed for attachment of phagosomes to lysosomes. Rather, Rab7 may anchor Vps34 to (phago)lysosome membranes and provide PI(3)P (Stein *et al.*, 2003, Jeschke *et al.*, 2015), which we here show is dispensable for phagosome-to-lysosome binding yet necessary for PLF. Phagosome-to-lysosome binding required PI(4)P as judged by its sensitivity to P4C. Moreover, binding was inhibited by 4C5G, an antibody that inhibits class II PI4K activity (Endemann *et al.*, 1991) and generation of PI(4)P in (phago)lysosome membranes (Jeschke *et al.*, 2015). Class II PI4Ks require ATP to generate PI(4)P from PI. As we show here, this requirement accounts at least in part for the ATP dependence of phagosome-to-lysosome binding.

PI(3)P and PI(4)P mediate distinct posttethering subreactions of PLF

We hypothesized that if PI(4)P was required to only link phagosomes and lysosomes then tethering and fusion should become independent of PI(4)P if membranes were tethered in an alternative way. Such alternative tether is PEG. Here PEG overcame the requirement for PI(4)P in phagosome-to-lysosome binding but not in the overall process of PLF. This observation suggested that PLF entails a second PI(4)P-dependent step after tethering, a hypothesis that is supported by further lines of evidence: 1) phagosome-to-lysosome binding was less sensitive to a PI(4)P-binding domain than content mixing, 2) the overall process of PLF remained sensitive to a PI(4)P-binding domain even after completion of phagosome-to-lysosome binding, and 3) content mixing between phagosomes and lysosomes never became resistant toward a PI(4)P-binding domain. Altogether these data provide compelling evidence for a late requirement of PI(4)P in PLF.

We have observed that PI(3)P acts after tethering but before a second PI(4)P requirement. Hence, PI(3)P and PI(4)P regulate

different posttethering steps of PLF. For PI(3)P, these might correspond to *trans*-SNARE complex assembly or hemifusion and for PI(4)P to hemifusion or fusion. In yeast vacuole fusion, *trans*-SNARE complex assembly and hemifusion follow each other quickly and occur long before content mixing (Jun and Wickner, 2007). Moreover, the overall reaction never acquires resistance toward content-mixing inhibitors (Reese and Mayer, 2005). In line with this, the clear kinetic difference of PLF inhibition by PI(3)P or PI(4)P binders might imply that PI(4)P is required for fusion per se, whereas PI(3)P is required for SNARE pairing or hemifusion.

At low concentrations (<5% [wt/vol]) PEG promotes tethering and *trans*-SNARE complex assembly, but it cannot bypass the requirement of fusion for SNARE pairing (Dennison *et al.*, 2006; Furukawa and Mima, 2014). In the presence of PEG, PLF was less sensitive toward a PI(3)P-sequestering protein domain. Given that PEG action cannot functionally replace *trans*-SNARE complex assembly, this implies that, upon sequestration of PI(3)P, SNARE proteins pair but do not trigger lipid mixing. Hence, PI(3)P could contribute to the recruitment of SM proteins (e.g., the HOPS complex subunit Vps33A [Baker *et al.*, 2015]) or of factors that eventually provoke fusion through insertion of hydrophobic wedge domains in the vicinity of *trans*-SNARE complexes, for example, α-SNAP or synaptotagmin (Zick *et al.*, 2015; Wickner and Rizo, 2017).

PI(3)P and PI(4)P anchor Arl8 and the HOPS complex to (phago)lysosome membranes

Membrane fusion requires that fusion-relevant factors are assembled into membrane microdomains at future fusion sites at the right time. Given their function as short-lived signposts for the membrane recruitment and/or activation of proteins, PIPs are exquisitely suited as organizers of such microdomains. PI(4)P could contribute to phagosome-lysosome tethering by recruiting HOPS. HOPS binds to PIPs including PI(4)P (Stroupe *et al.*, 2006) and to RILP (van der Kant *et al.*, 2013), which is released from late phagosomes and endosomes when PI(4)P is depleted (Levin *et al.*, 2017).

We now report that sequestration of PI(4)P did not only inhibit phagosome-to-lysosome binding but also removed Arl8 and its interactor, the HOPS complex subunit Vps41 from the membranes. Possibly, PI(4)P anchors Arl8 to (phago)lysosomes, and HOPS is removed along with Arl8. Whether binding of Arl8 to (phago)lysosomes is direct or whether it depends on BLOC-one-related complex (BORC), a multi-subunit protein complex implicated in membrane targeting of Arl8 (Pu *et al.*, 2015) that may bind to PI(4)P remains to be determined.

Given that Arl8 can recruit HOPS to lysosomes (Khatter *et al.*, 2015), it was surprising that membrane localization of HOPS and of Arl8 were uncoupled: omitting ATP from reaction mixtures decreased (phago)lysosome levels of Arl8 but not of Vps41/HOPS, and addition of 2xFYVE domain decreased levels of Vps41/HOPS but not of Arl8. These observations suggested that (i) in "no ATP" samples, HOPS interactors such as PLEKHM1 (Marwaha *et al.*, 2017), RILP (van der Kant *et al.*, 2013), and/or Syntaxin 7 (Kim *et al.*, 2001) can preserve membrane association of HOPS, even when Arl8 is absent, and that (ii) HOPS associates with (phago)lysosomes by binding to PI(3)P and/or PI(4)P directly or indirectly via PLEKHM1. The latter may well be the case as PLEKHM1 possesses two PH domains, whose lipid-binding specificities, however, remain to be determined (McEwan *et al.*, 2015).

PIP-dependent binding of Arl8 and HOPS to (phago)lysosomes: implications for the mechanism of PLF

Strikingly and different from homotypic yeast vacuole fusion, membrane association of HOPS did not correlate with membrane tethering. Given that previous reports have assigned HOPS functions in tethering (Hickey and Wickner, 2010) and *trans*-SNARE complex (Baker *et al.*, 2015; Orr *et al.*, 2017) assembly and proofreading (Starai *et al.*, 2008), our data suggest that HOPS regulates PLF at the level of *trans*-SNARE–promoted docking rather than tethering.

Membrane association of Arl8, by contrast, correlated well with phagosome-to-lysosome binding, suggesting that, in contrast to HOPS, Arl8 is necessary for tethering. Possibly, PLEKHM1 can mediate phagosome-to-lysosome binding in the absence of HOPS by linking Arl8 and Rab7 (Marwaha *et al.*, 2017). This would fit with our observation that 2xFYVE removed Vps41/HOPS from (phago)lysosomes yet did not affect levels of Arl8 and Rab7.

In this basic study, we attributed PI(3)P and PI(4)P to defined subreactions of PLF and identified these PIPs as membrane association cues of established regulators of late endocytic trafficking, that is, Arl8 and its effector HOPS. In our working model (Figure 8), PI(4)P on phagosomes mediates recruitment of Arl8 and promotes tethering to lysosomes. Then PI(3)P and PI(4)P cooperatively recruit HOPS, which supports tethering, guides the formation of cognate *trans*-SNARE complexes, and, eventually, promotes content mixing between phagosomes and lysosomes.

Previous microscopic and protein binding studies have identified a complex machinery of various multiply interacting proteins (e.g., Arl8, Rab7, RILP, PLEKHM1, and HOPS) as required for fusion of lysosomes with endosomes, autophagosomes, and phagosomes. Functional assays, such as the ones developed here, may now help to determine the precise hierarchy of interactions between fusion-relevant proteins and lipids and yield a holistic picture of how lysosomes fuse with phagosomes and other compartments.
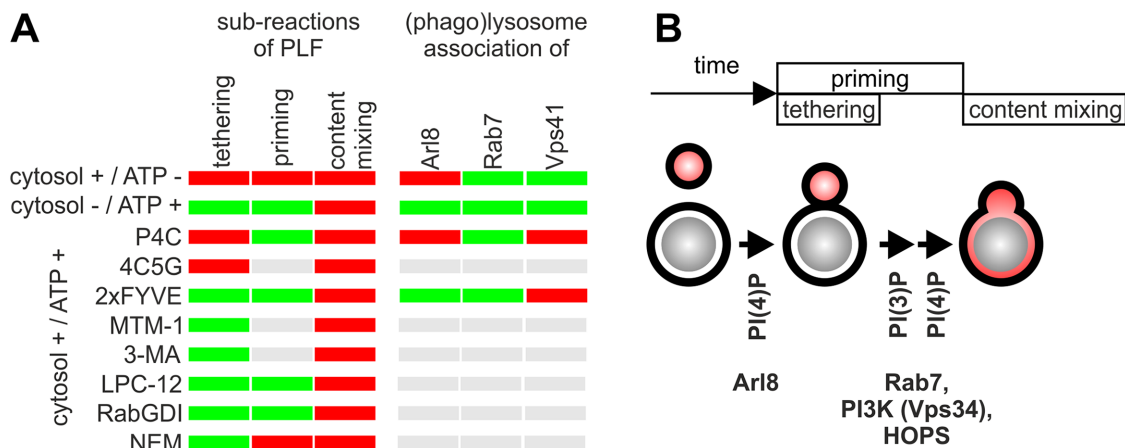
FIGURE 8: Data summary. (A) Schematic representation of which subreactions of PLF are inhibited and which proteins are displaced from (phago)lysosomes by the indicated reagents. Red boxes indicate sensitivity to or displacement by a reagent; green boxes indicate resistance or no displacement. Given that priming was not inhibited by sequestration of PI(3)P or by PI(4)P, inhibitors of PI3K or PI4K and the PI(3)P-phosphatase MTM-1 were not tested, as indicated by the gray boxes. Tethering was assayed as attachment of lysosomes to phagosomes. Priming was assayed by analysis of α-SNAP release from (phago)lysosome membranes, and content mixing by microscopic evaluation of transfer of a fluorescent tracer from lysosomes to phagosomes. (Phago)lysosome association of proteins indicated was analyzed by immunoblotting. (B) Working model for the sequence and PIP requirements of PLF subreactions. Tethering precedes or is independent of priming. PI(4)P is required for tethering and a second step after tethering. PI(3)P is required after tethering but before the second PI(4)P-dependent step. Priming does not require PI(3)P or PI(4)P. Analysis of (phago)lysosome levels of Arl8, Rab7, and HOPS under conditions specified in A suggested that Arl8 is required for PI(4)P-dependent tethering, whereas HOPS is required for PI(3)P- and PI(4)P-dependent content mixing. Given that RabGDI, RILP-C33, and PI3K inhibitors block the overall process of PLF, but do not affect phagosome-to-lysosome binding, Rab7 and PI3K (Vps34) have been assigned to a subreaction following tethering.

MATERIALS AND METHODS

Chemicals and reagents

All chemicals were of research grade. ATP (no. 50-720-651), creatine kinase (no. 10127566001), and creatine phosphate (no. 621714) were from Roche. 3-MA (no. M2981), 5(6)-carboxytetramethylrhodamine (no. 21953), NEM (no. E3876), and PEG3350 (no. P4338) were from Sigma. Glutathione sepharose 4B was from GE Healthcare (no. 17-0756-01). Ni-NTA-Agarose was from Qiagen (no. 30210). Proteinase K was from Roth (no. 7528.2). Carboxylate 1 μm microspheres were from Polysciences (no. 08228). NeutrAvidin biotin-binding protein (no. 31000) and EZ-Link Sulfo-NHS-LC-Biotin (no. 21327) were from Thermo Fisher Scientific. Cy5-NHS ester was from lumiprobe (no. 43020).

Rabbit anti-GST (no. sc-459), mouse anti-α/β-SNAP (no. sc-48349), mouse anti-Vps41 (no. sc-377118), and mouse anti-Arl8 a/b (sc-398635) were from Santa Cruz Biotechnology. Goat anti-rabbit Alexa 488 was from Life technologies (no. A11008). Rabbit anti-Rab7 was provided by T. Watts (University of Toronto, Toronto, ON, Canada; Bertram *et al.*, 2002). LPC-12 was from Avanti Polar Lipids (no. 855475P).

Purified inhibitory mouse anti-type II PI4K (clone 4C5G) was as previously published (Endemann *et al.*, 1991). F_{ab} fragments of 4C5G were prepared using the Mouse IgG1 F_{ab} and $F(_{ab}')2$ preparation kit (Pierce, no. 44680). Rat anti-murine lysosome-associated membrane protein 1 (LAMP1; clone 1D4B) developed by J. T. August was obtained from the Developmental Studies Hybridoma Bank under the auspices of the Eunice Kennedy Shriver National Institute of Child Health and Human Development and maintained by the University of Iowa (Department of Biology, Iowa City, IA).

Plasmids and purification of recombinant proteins

Expression plasmids for 2xFYVE-GST (two copies of FYVE [Fab1p, YOTB, Vac1p, EEA1] domain from Hrs [hepatocyte growth factor-regulated tyrosine kinase substrate] in tandem) (Gillooly *et al.*, 2000) and hexahistidine- and GST-tagged MTM1 (Taylor *et al.*, 2000) were from W. Wickner (Geisel School of Medicine, Dartmouth College, Hanover, NH). Plasmids for expression of hexahistidine fusions of RabGDI (Ullrich *et al.*, 1993) were provided by O. Ullrich (Hamburg University of Applied Sciences, Hamburg, Germany). Plasmids encoding GST fusions of SidC P4C (PI(4)P-binding fragment from *Legionella pneumophila* SidC) were provided by H. Hilbi (Institute of Medical Microbiology, University of Zürich, Zürich, Switzerland) (Ragaz *et al.*, 2008). All DNA contructs were validated by nucleotide sequencing. Plasmids encoding a GST fusion of RILP-C33 were provided by C. Bucci (Department of Biological and Environmental Sciences and Technologies [DiSTeBA], University of Salento, Lecce, Italy) (Cantalupo *et al.*, 2001).

The recombinant proteins were expressed in *Escherichia coli* BL21(DE3) (genotype: *fhuA2 [lon] ompT gal (λ DE3) [dcm] ΔhsdS λ DE3 = λ sBamHIo ΔEcoRI-B int::(lacI::PlacUV5::T7 gene1) i21 Δnin5*). For expression of plasmid-encoded recombinant proteins, 20 ml of lysogeny broth (LB) broth containing 100 μg/ml either ampicillin or kanamycin was inoculated with transformed bacteria and incubated on a rocker for 16 h at 200 rpm and 37°C. The resulting culture was diluted in 1 l of LB broth containing the respective antibiotic and incubated until it reached an optical density at 600 nm (OD_{600}) of 0.5. Isopropyl-β-D-galactoside (IPTG) was added to a final concentration of 0.25 mM, and the culture was incubated for 16 h at 200 rpm and 16°C. Bacteria were harvested (10 min, $6000 \times g$, 4°C), resuspended in hexahistidine lysis buffer (50 mM NaH_2PO_4, 300 mM NaCl, 10 mM imidazole, 5% [vol/vol] glycerol, pH 8.0) or in phosphate-buffered saline (PBS) (for GST-tagged proteins) containing 1×

protease inhibitor cocktail (PIC), and homogenized by sonication at 4°C. Homogenates were centrifuged (30 min, $14,000 \times g$, 4°C), and supernatants were subjected to affinity chromatography using Ni-NTA agarose or glutathione sepharose.

For purification of hexahistidine-tagged proteins, 10 ml of the homogenate was mixed with Ni-NTA agarose (1 ml slurry) and incubated for 30 min at 4°C on an end-over-end shaker. Ni-NTA agarose was washed once in 10 ml hexahistidine lysis buffer and twice in 10 ml hexahistidine wash buffer (50 mM NaH_2PO_4, 300 mM NaCl, 20 mM imidazole, 5% [vol/vol] glycerol, pH 8.0) (1 min, 1800 $\times g$, 4°C), and bound proteins were eluted with hexahistidine elution buffer (50 mM NaH_2PO_4, 300 mM NaCl, 250 mM imidazole, 5% [vol/vol] glycerol, pH 8.0).

For purification of GST-tagged proteins, homogenates containing the protein of interest were mixed with glutathione sepharose (0.3 ml slurry per 10 ml homogenate) and incubated for 30 min at 4°C on an end-over-end shaker. Glutathione sepharose was washed thrice in 10 ml PBS (1 min, $1800 \times g$, 4°C), and bound proteins were eluted with GST elution buffer (50 mM Tris, 10 mM glutathione, pH 7.5). Recombinant proteins were dialyzed against homogenization buffer (HB; 250 mM sucrose, 20 mM HEPES, 0.5 mM ethylene glycol-bis(β-aminoethyl ether)-*N,N,N',N'*-tetraacetic acid [EGTA], pH 7.2) for 16 h at 4°C, snap-frozen in liquid nitrogen, and stored at –80°C.

Cultivation of cells

High mannose receptor cell line J774E (Fiani *et al.*, 1998) from P. D. Stahl (Washington University in St. Louis, St. Louis, MO) was cultivated in DMEM containing 10% (vol/vol) fetal calf serum (Life Technologies) at 37°C in a humid atmosphere of 7% CO_2. Cells were confirmed to be mycoplasma free by PCR (forward primer: 5′-CACCATCTGTCACTCTGTTAACC-3′, reverse primer: 5′-GGAGCAAACAGGATTAGATACCC-3′). Cells were of mouse origin as validated by PCR according to Cooper *et al.* (2007).

Purification of phagosomes and lysosomes

Endocytic compartments were labeled with BSA-rhodamine-biotin (BSA-rho-bio) and ferrofluid. For preparation of BSA-rho-bio, 5 mg/ml BSA in 0.1 M $NaHCO_3$ was mixed with 1.2 mg/ml 5(6)-carboxytetramethylrhodamine *N*-hydroxysuccinimide (NHS) ester and 1.56 mg/ml biotin-LC-NHS-ester, incubated for 2 h at ambient temperature (AT), and dialyzed against PBS for 2 h. Per 10-cm cell culture dish used for lysosome preparation, 30 μl ferrofluid was adjusted to 300 μl PBS and 10 mg/ml BSA, sonicated, incubated for 16 h on a rocker at 4°C, sonicated again, passed through a 0.2-μm-pore-size sterile filter, and mixed with 2.5 ml DMEM/fetal calf serum (FCS).

For labeling with BSA-rho-bio, cells were incubated for 16 h at 37°C in DMEM/FCS containing 100 μg/ml BSA-rho-bio. Fluor-containing DMEM/FCS was removed, and 2.5 ml of the ferrofluid suspension in DMEM/FCS was added. After 30 min at 37°C ("pulse"), cells were rinsed twice in PBS, new DMEM/FCS was added, and cells were incubated for 120 min at 37°C ("chase").

Ferrofluid-containing endocytic compartments were purified as previously described (Jeschke *et al.*, 2015). DMEM/FCS was discarded, PBS was added, and cells were harvested using a cell scraper. Cells were washed sequentially in PBS/5 mM EDTA and HB (7 min, $160 \times g$, 4°C), resuspended in HB containing 1× PIC, and homogenized in a dounce homogenizer. A postnuclear supernatant (PNS) was prepared (5 min, $800 \times g$, 4°C), diluted in HB (approximately 500 μl per culture dish [Ø 10 cm] used for endosome preparation), and incubated for 30 min at 4°C on a Dynal magnetic rack. Supernatants were removed, and endocytic compartments were collected.

To coat carboxylate-modified 1-µm latex beads with NeutrAvidin biotin-binding protein, 4.6×10^{10} particles/ml were washed twice in MES buffer (50 mM MES/NaOH, pH 6.8; $16,100 \times g$, 5 min, AT), resuspended in MES buffer containing 0.3 mg/ml NeutrAvidin, and incubated on a rocker for 15 min; 1-ethyl-3-(3-dimethylaminopropyl) carbodiimide hydrochloride (EDAC) was added to a final concentration of 0.1 mM. After 60 min at AT, the bead suspension was adjusted to 0.2 mM EDAC and incubated for additional 60 min. Tris buffer (1.5 M, Tris-HCl, pH 8.8) was added to a final concentration of 10 mM. Particles were washed thrice in PBS (5 min, $16,100 \times g$, 4°C), resuspended in storage buffer (PBS, 10 mg/ml BSA, 1× PIC, 0.01% NaN$_3$), and stored at 4°C. In some experiments (Figures 2 and 6), Cy5-labeled latex beads were used. NeutrAvidin-coated beads were sedimented by centrifugation ($16,100 \times g$, 5 min, AT) and resuspended in 0.1 M NaHCO$_3$. Cy5-NHS ester was added to a final concentration of 5 µg/ml and beads were incubated on a rocker (30 min, AT). Tris buffer (1.5 M, Tris-HCl, pH 8.8) was added to a final concentration of 10 mM Tris, and beads were sedimented by centrifugation (5 min, $16,100 \times g$, 4°C).

Purification of latex bead phagosomes (LBPs) from J774E cells was done as in described previously (Jeschke et al., 2015). LBP preparations of different maturation stages were obtained using different pulse/chase protocols: Late phagosomes were prepared after 10 min/20 min (pulse/chase) and phagolysosomes after 30 min/60 min. DMEM/FCS was discarded, PBS was added, and cells were harvested using a cell scraper. Cells were washed sequentially in PBS/5 mM EDTA and HB ($160 \times g$, 4°C, 7 min), resuspended in HB containing 1× PIC, and homogenized in a dounce homogenizer. A PNS was prepared (5 min, $800 \times g$, 4°C), adjusted to 35% sucrose by addition of an equal volume of HB containing 62% (wt/vol) sucrose, overlayed with 5 ml of HB containing 25% (wt/vol) sucrose, and 3 ml of HB. After centrifugation in a SW40 Ti rotor (30 min, $42,000 \times g$, 4°C), LBPs were harvested from the 25%/HB interface.

Cell-free assay of phagosome–lysosome fusion or tethering
BSA-biotin was prepared by mixing 5 mg/ml BSA in 0.1 M NaHCO$_3$ with 1.56 mg/ml biotin-LC-NHS-ester for 2 h at AT and subsequent dialysis against HB (2 h, AT).

To prepare a cytosol fraction from J774E macrophages, cells from 50 confluent dishes (Ø 10 cm) were harvested using a cell scraper and washed sequentially in PBS, PBS/5 mM EDTA, and twice in HB (7 min, $160 \times g$, 4°C). Cells were resuspended in 2 ml HB containing 1× PIC and homogenized in a dounce homogenizer. The homogenate was centrifuged (60 min, $100,000 \times g$, 4°C), and supernatants were collected and centrifuged again (5 min, $16,100 \times g$, 4°C). Supernatants (cytosol) were snap-frozen in liquid nitrogen and stored at –80°C.

Cell-free fusion of latex bead phagosomes (LBPs) with lysosomes was performed as described with modifications (Jeschke et al., 2015). LBPs contained NeutrAvidin-coated 1-µm latex particles and lysosomes were fluid phase-labeled by BSA-rho-bio. Phagosome-lysosome fusion resulted in colocalization between the phagocytic probe and the lysosome tracer and was quantified by fluorescence microscopy. Conjugation of avidin to latex particles and of biotin to BSA-rho served to ensure that phagosomes retained lysosomal tracer after fusion, even if they were lysed prior to microscopic analysis. To avoid fusion-independent binding of BSA-rho-bio released from endocytic compartments to latex particles (i.e., permeabilized phagosomes), fusion reactions were supplemented with excess BSA-bio which blocks accessible biotin-binding sites on latex beads.

A cell-free fusion reaction contained 0.625 OD$_{600}$/ml purified LBPs, 0.4 mg/ml lysosomes, 0.12 mg/ml BSA-biotin, and 2 mg/ml

macrophage cytosol, 1× ATP-regenerating system, 1× salts, and 1 mM DTT in a total volume of 30 µl (Jeschke et al., 2015). After 60 min at 37°C, reactions were set on ice, proteinase K was added to a final concentration of 0.2 mg/ml for 15 min, 1.75 mg/ml phenylmethanesulfonyl fluoride was added, and reactions were adjusted to a volume of 200 µl by addition of HB. Reaction mixtures were layered on top of 1 ml HB/25% (wt/vol) sucrose cushions and centrifuged (30 min, $1800 \times g$, 4°C) in a swing-out rotor. LBPs were collected from the HB/25% (wt/vol) sucrose/HB interface, adjusted to 2 mg/ml BSA, spun onto glass coverslips (15 min, $690 \times g$, 4°C), and fixed for 16 h at 4°C in 4% FA in HB. Samples were mounted in Mowiol and analyzed by fluorescence microscopy using Zeiss AxioPlan epifluorescence microscope. All coverslips were anonymized. Colocalization of LBPs with lysosomal BSA-rho-bio, indicative of LBP-lysosome fusion, was quantified microscopically from at least 300 LBPs. Under standard fusion conditions, 3.57–37.3% (15.0 ± 7.95, mean ± SD; $n = 37$) of LBPs colocalized with the lysosome tracer. To facilitate averaging, colocalization in standard reactions was set as a 100% unless stated otherwise.

To quantify phagosome-to-lysosome binding, cell-free reactions as above were supplemented with 100 µM LPC-12. After 60 min at 37°C, reactions were set on ice, adjusted to 35% (wt/vol) sucrose by adding 30 µl of 62% (wt/vol) sucrose solution, overlaid with 1 ml 25% (wt/vol) sucrose solution and 200 µl of HB. Density gradients were centrifuged (30 min, $1800 \times g$, 4°C) in a swing-out rotor. LBPs were collected from the HB/25% (wt/vol) sucrose/HB interface, adjusted to 2 mg/ml BSA, spun onto glass coverslips (15 min, $690 \times g$, 4°C), and fixed for 16 h at 4°C in 4% FA in HB. Samples were mounted in Mowiol and analyzed by fluorescence microscopy. All coverslips were anonymized. The percentage of LBPs that were bound to at least one lysosome was determined from at least 200 LBPs.

Assay of lysosome leakiness
Fusion reactions of twice the standard volume were incubated for 60 min at 37°C in the presence or absence of 100 µM LPC-12 and/or 1% (vol/vol) Triton X-100 (TX-100) as indicated, set on ice, and adjusted to 100 µl volume by addition of HB. Compartments were sedimented by centrifugation ($16,100 \times g$, 30 min, 4°C), and supernatants were collected. Supernatants were adjusted to 1% (vol/vol) TX-100 and assayed for leaked BSA-rho-bio fluorescence in a FLx800 microplate fluorometer (Biotek Instruments GmbH) at 560 (± 20) nm excitation and 625 (±16) nm emission. Fluorescence signals emitted on excitation of HB containing 1% (vol/vol) TX-100 were substracted from all samples.

Assay of α-SNAP release and displacement of Vps41 and Arl8
Fusion reactions of twice the standard volume were incubated under conditions specified in figure legends (Figure 1, Supplemental Figure S3, Figure 7, and Supplemental Figure S4). Reactions were stopped by addition of 1 ml of cold HB. Phagosomes and lysosomes were sedimented by centrifugation ($16,000 \times g$, 30 min, 4°C), resuspended in 20 µl 1× SDS sample buffer, and analyzed for LAMP1 and α-SNAP or for LAMP1, Vps41, Arl8, and Rab7 by SDS–PAGE and immunoblotting. Immunoblots were quantified using ImageJ image processing software.

Staining of PI(3)P and PI(4)P on tethered phagosomes and lysosomes
Purified phagosomes and lysosomes were incubated under fusion assay conditions in the presence of 2 µM of GST-tagged lipid probes

or 2 μM GST and 100 μM LPC-12 for 60 min. Reactions were adjusted to 35% sucrose by addition of HB/62% wt/vol sucrose and overlayed with 1 ml of HB/25% (wt/vol) sucrose and 200 μl of HB, and density gradients were centrifuged for 30 min at $1800 \times g$ and 4°C in a swing-out rotor. LBPs were harvested from the HB/25% (wt/vol) sucrose/HB interface, adjusted to 500 μl HB and 2 mg/ml BSA, spun onto glass coverslips (15 min, $690 \times g$, 4°C), and fixed for 16 h at 4°C in 4% FA in HB.

Fixative was quenched for 30 min at AT in HB/50 mM NH_4Cl and IF blocking buffer (PBS/4% [wt/vol] BSA) was added for 30 min. For detection of GST-tagged lipid probes, samples were stained with a rabbit anti-GST antibody (1:200 in IF blocking buffer) and an Alexa488-conjugated secondary antibody (1:200 in IF blocking buffer). Immunostaining was performed at AT and by adding 30 μl antibody solution per coverslip. Coverslips were incubated with primary antibodies for 60 min, rinsed five times in PBS, incubated with secondary antibodies for 30 min, rinsed five times in PBS, and were mounted in Mowiol. Samples were analyzed using Zeiss Axio Observer.Z1 epifluorescence microscope.

Curve fitting and statistics

Exponential and sigmoid curve fits were determined in PTC Mathcad 14 according to the least-squares method. All data are means ± SEM from at least three independent experiments. Data were analyzed by the two-tailed unpaired Student's t test with significance assumed at $p < 0.05$ (*) and high significance at $p < 0.01$ (**). The exact p values and numbers of independent experiments are given in the supporting information section.

REFERENCES

Alvarez-Dominguez C, Barbieri AM, Berón W, Wandinger-Ness A, Stahl PD (1996). Phagocytosed live Listeria monocytogenes influences Rab5-regulated in vitro phagosome-endosome fusion. J Biol Chem 271, 13834–13843.

Baker RW, Jeffrey PD, Zick M, Phillips BP, Wickner WT, Hughson FM (2015). A direct role for the Sec1/Munc18-family protein Vps33 as a template for SNARE assembly. Science 349, 1111–1114.

Bakowski MA, Braun V, Lam GY, Yeung T, Heo WD, Meyer T, Finlay BB, Grinstein S, Brumell JH (2010). The phosphoinositide phosphatase SopB manipulates membrane surface charge and trafficking of the Salmonella-containing vacuole. Cell Host Microbe 7, 453–462.

Becken U, Jeschke A, Veltman K, Haas A (2010). Cell-free fusion of bacteria-containing phagosomes with endocytic compartments. Proc Natl Acad Sci USA 107, 20726–20731.

Bertram EM, Hawley RG, Watts TH (2002). Overexpression of rab7 enhances the kinetics of antigen processing and presentation with MHC class II molecules in B cells. Int Immunol 14, 309–318.

Cantalupo G, Alifano P, Roberi V, Bruni CB, Bucci C (2001). Rab-interacting lysosomal protein (RILP): the Rab7 effector required for transport to lysosomes. EMBO J 20, 683–693.

Carlton JG, Cullen PJ (2005). Coincidence detection in phosphoinositide signaling. Trends Cell Biol 15, 540–547.

Cheever ML, Sato TK, Beer T, Kutateladze TG, Emr SD, Overduin M (2001). Phox domain interaction with PtdIns(3)P targets the Vam7 t-SNARE to vacuole membranes. Nat Cell Biol 3, 613–618.

Christoforidis S, McBride HM, Burgoyne RD, Zerial M (1999). The Rab5 effector EEA1 is a core component of endosome docking. Nature 397, 621–625.

Collins RF, Schreiber AD, Grinstein S, Trimble WS (2002). Syntaxins 13 and 7 function at distinct steps during phagocytosis. J Immunol 169, 3250–3256.

Colombo MI, Gelberman SC, Whiteheart SW, Stahl PD (1998). N-ethylmaleimide-sensitive factor-dependent alpha-SNAP release, an early event in the docking/fusion process, is not regulated by Rab GTPases. J Biol Chem 273, 1334–1338.

Colucci AM, Campana MC, Bellopede M, Bucci C (2005). The Rab-interacting lysosomal protein, a Rab7 and Rab34 effector, is capable of self-interaction. Biochem Biophys Res Commun 334, 128–133.

Cooper JK, Sykes G, King S, Cottrill K, Ivanova NV, Hanner R, Ikonomi P (2007). Species identification in cell culture: a two-pronged molecular approach. In Vitro Cell Develop Biol Animal 43, 344–351.

Dai S, Zhang Y, Weimbs T, Yaffe MB, Zhou D (2007). Bacteria-generated PtdIns(3)P recruits VAMP8 to facilitate phagocytosis. Traffic 8, 1365–1374.

De Matteis MA, Godi A (2004). PI-loting membrane traffic. Nat Cell Biol 6, 487–492.

Dennison MS, Bowen ME, Brunger AT, Lentz BR (2006). Neuronal SNAREs do not trigger fusion between synthetic membranes but do promote PEG-mediated membrane fusion. Biophys J 90, 1661–1675.

Desjardins M, Huber LA, Parton RG, Griffiths G (1994). Biogenesis of phagolysosomes proceeds through a sequential series of interactions with the endocytic apparatus. J Cell Biol 124, 677–688.

Endemann GC, Graziani A, Cantley LC (1991). A monoclonal antibody distinguishes two types of phosphatidylinositol 4-kinase. Biochem J 273, 63–66.

Fasshauer D, Sutton RB, Brunger AT, Jahn R (1998). Conserved structural features of the synaptic fusion complex: SNARE proteins reclassified as Q- and R-SNAREs. Proc Natl Acad Sci USA 95, 15781–15786.

Fiani ML, Beitz J, Turvy D, Blum JS, Stahl PD (1998). Regulation of mannose receptor synthesis and turnover in mouse J774 macrophages. J Leukoc Biol 64, 85–91.

Flannagan RS, Jaumouillé V, Grinstein S (2012). The cell biology of phagocytosis. Annu Rev Pathol 7, 61–98.

Furukawa N, Mima J (2014). Multiple and distinct strategies of yeast SNAREs to confer the specificity of membrane fusion. Sci Rep 4, 4277.

Garg S, Sharma M, Ung C, Tuli A, Barral DC, Hava DL, Veerapen N, Besra GS, Hacohen N, Brenner MB (2011). Lysosomal trafficking, antigen presentation, and microbial killing are controlled by the Arf-like GTPase Arl8b. Immunity 35, 182–193.

Geumann U, Barysch SV, Hoopmann P, Jahn R, Rizzoli SO (2008). SNARE function is not involved in early endosome docking. Mol Biol Cell 19, 5327–5337.

Gillooly DJ, Morrow IC, Lindsay M, Gould R, Bryant NJ, Gaullier JM, Parton RG, Stenmark H (2000). Localization of phosphatidylinositol 3-phosphate in yeast and mammalian cells. EMBO J 19, 4577–4588.

Grosshans BL, Ortiz D, Novick P (2006). Rabs and their effectors: achieving specificity in membrane traffic. Proc Natl Acad Sci USA 103, 11821–11827.

Harrison RE, Bucci C, Vieira OV, Schroer TA, Grinstein S (2003). Phagosomes fuse with late endosomes and/or lysosomes by extension of membrane protrusions along microtubules: role of Rab7 and RILP. Mol Cell Biol 23, 6494–6506.

Hernandez JM, Stein A, Behrmann E, Riedel D, Cypionka A, Farsi Z, Walla PJ, Raunser S, Jahn R (2012). Membrane fusion intermediates via directional and full assembly of the SNARE complex. Science 336, 1581–1584.

Hickey CM, Wickner W (2010). HOPS initiates vacuole docking by tethering membranes before trans-SNARE complex assembly. Mol Biol Cell 21, 2297–2305.

Hong W, Lev S (2014). Tethering the assembly of SNARE complexes. Trends Cell Biol 24, 35–43.

Jahraus A, Tjelle TE, Berg T, Habermann A, Storrie B, Ullrich O, Griffiths G (1998). In vitro fusion of phagosomes with different endocytic organelles from J774 macrophages. J Biol Chem 273, 30379–30390.

Jeschke A, Zehethofer N, Lindner B, Krupp J, Schwudke D, Haneburger I, Jovic M, Backer JM, Balla T, Hilbi H, Haas A (2015). Phosphatidylinositol 4-phosphate and phosphatidylinositol 3-phosphate regulate phagolysosome biogenesis. Proc Natl Acad Sci USA 112, 4636–4641.

Jun Y, Wickner W (2007). Assays of vacuole fusion resolve the stages of docking, lipid mixing, and content mixing. Proc Natl Acad Sci USA 104, 13010–13015.

Khatter D, Raina VB, Dwivedi D, Sindhwani A, Bahl S, Sharma M (2015). The small GTPase Arl8b regulates assembly of the mammalian HOPS complex on lysosomes. J Cell Sci 128, 1746–1761.

Kim BY, Krämer H, Yamamoto A, Kominami E, Kohsaka S, Akazawa C (2001). Molecular characterization of mammalian homologues of class C Vps proteins that interact with syntaxin-7. J Biol Chem 276, 29393–29402.

Kinchen JM, Doukoumetzidis K, Almendinger J, Stergiou L, Tosello-Trampont A, Sifri CD, Hengartner MO, Ravichandran KS (2008). A pathway for phagosome maturation during engulfment of apoptotic cells. Nat Cell Biol 10, 556–566.

Kutateladze TG (2010). Translation of the phosphoinositide code by PI effectors. Nat Chem Biol 6, 507–513.

Levin R, Hammond GRV, Balla T, De Camilli P, Fairn GD, Grinstein S (2017). Multiphasic dynamics of phosphatidylinositol 4-phosphate during phagocytosis. Mol Biol Cell 28, 128–140.

Lin X, Yang T, Wang S, Wang Z, Yun Y, Sun L, Zhou Y, Xu X, Akazawa C, Hong W, Wang T (2014). RILP interacts with HOPS complex via Vps41 subunit to regulate endocytic trafficking. Sci Rep 4, 7282.

Marwaha R, Arya SB, Jagga D, Kaur H, Tuli A, Sharma M (2017). The Rab7 effector PLEKHM1 binds Arl8b to promote cargo traffic to lysosomes. J Cell Biol 216, 1051–1070.

Mayer A, Scheglmann D, Dove S, Glatz A, Wickner W, Haas A (2000). Phosphatidylinositol 4,5-bisphosphate regulates two steps of homotypic vacuole fusion. Mol Biol Cell 11, 807–817.

Mayer A, Wickner W (1997). Docking of yeast vacuoles is catalyzed by the Ras-like GTPase Ypt7p after symmetric priming by Sec18p (NSF). J Cell Biol 136, 307–317.

Mayer A, Wickner W, Haas A (1996). Sec18p (NSF)-driven release of Sec17p (alpha-SNAP) can precede docking and fusion of yeast vacuoles. Cell 85, 83–94.

Mayorga LS, Bertini F, Stahl PD (1991). Fusion of newly formed phagosomes with endosomes in intact cells and in a cell-free system. J Biol Chem 266, 6511–6517.

McEwan DG, Popovic D, Gubas A, Terawaki S, Suzuki H, Stadel D, Coxon FP, Miranda de Stegmann D, Bhogaraju S, Maddi K, et al. (2015). PLEKHM1 regulates autophagosome-lysosome fusion through HOPS complex and LC3/GABARAP proteins. Mol Cell 57, 39–54.

Melia TJ, You D, Tareste DC, Rothman JE (2006). Lipidic antagonists to SNARE-mediated fusion. J Biol Chem 281, 29597–29605.

Mukherjee K, Siddiqi SA, Hashim S, Raje M, Basu SK, Mukhopadhyay A (2000). Live Salmonella recruits N-ethylmaleimide-sensitive fusion protein on phagosomal membrane and promotes fusion with early endosome. J Cell Biol 148, 741–753.

Mullock BM, Bright NA, Fearon CW, Gray SR, Luzio JP (1998). Fusion of lysosomes with late endosomes produces a hybrid organelle of intermediate density and is NSF dependent. J Cell Biol 140, 591–601.

Orr A, Song H, Rusin SF, Kettenbach AN, Wickner W (2017). HOPS catalyzes the interdependent assembly of each vacuolar SNARE into a SNARE complex. Mol Biol Cell 28, 975–983.

Peyron P, Maridonneau-Parini I, Stegmann T (2001). Fusion of human neutrophil phagosomes with lysosomes in vitro: involvement of tyrosine kinases of the Src family and inhibition by mycobacteria. J Biol Chem 276, 35512–35517.

Poccia D, Larijani B (2009). Phosphatidylinositol metabolism and membrane fusion. Biochem J 418, 233–246.

Pols MS, ten Brink C, Gosavi P, Oorschot V, Klumperman J (2013). The HOPS proteins hVps41 and hVps39 are required for homotypic and heterotypic late endosome fusion. Traffic 14, 219–232.

Pu J, Schindler C, Jia R, Jarnik M, Backlund P, Bonifacino JS (2015). BORC, a multisubunit complex that regulates lysosome positioning. Dev Cell 33, 176–188.

Ragaz C, Pietsch H, Urwyler S, Tiaden A, Weber SS, Hilbi H (2008). The Legionella pneumophila phosphatidylinositol-4 phosphate-binding type IV substrate SidC recruits endoplasmic reticulum vesicles to a replication-permissive vacuole. Cell Microbiol 10, 2416–2433.

Reese C, Mayer A (2005). Transition from hemifusion to pore opening is rate limiting for vacuole membrane fusion. J Cell Biol 171, 981–990.

Rusten TE, Stenmark H (2006). Analyzing phosphoinositides and their interacting proteins. Nat Methods 3, 251–258.

Sasaki T, Sasaki J, Sakai T, Takasuga S, Suzuki A (2007). The physiology of phosphoinositides. Biol Pharm Bull 30, 1599–1604.

Sasaki T, Takasuga S, Sasaki J, Kofuji S, Eguchi S, Yamazaki M, Suzukii A (2009). Mammalian phosphoinositide kinases and phosphatases. Prog Lipid Res 48, 307–343.

Shin OH, Lu J, Rhee JS, Tomchick DR, Pang ZP, Wojcik SM, Camacho-Perez M, Brose N, Machius M, Rizo J, et al. (2010). Munc13 C2B domain is an activity-dependent Ca2+ regulator of synaptic exocytosis. Nat Struc Mol Biol 17, 280–288.

Simonsen A, Lippé R, Christoforidis S, Gaullier JM, Brech A, Callaghan J, Toh BH, Murphy C, Zerial M, Stenmark H (1998). EEA1 links PI(3)K function to Rab5 regulation of endosome fusion. Nature 394, 494–498.

Starai VJ, Hickey CM, Wickner W (2008). HOPS proofreads the tans-SNARE complex for yeast vacuole fusion. Mol Biol Cell 19, 2500–2508.

Stein MP, Feng Y, Cooper KL, Welford AM, Wandinger-Ness A (2003). Human VPS34 and p150 are Rab7 interacting partners. Traffic 4, 754–771.

Stroupe C, Collins KM, Fratti RA, Wickner W (2006). Purification of active HOPS complex reveals its affinities for phosphoinositides and the SNARE Vam7p. EMBO J 25, 1579–1589.

Südhof TC, Rothman JE (2009). Membrane fusion: grappling with SNARE and SM proteins. Science 323, 474–477.

Taylor GS, Maehama T, Dixon JE (2000). Myotubularin, a protein tyrosine phosphatase mutated in myotubular myopathy, dephosphorylates the lipid second messenger, phosphatidylinositol 3-phosphate. Proc Natl Acad Sci USA 97, 8910–8915.

Ullrich O, Horiuchi H, Alexandrov K, Zerial M (1995). Use of Rab-GDP dissociation inhibitor for solubilization and delivery of Rab proteins to biological membranes in streptolysin O-permeabilized cells. Methods Enzymol 257, 243–253.

Ullrich O, Stenmark H, Alexandrov K, Huber LA, Kaibuchi K, Sasaki T, Takai Y, Zerial M (1993). Rab GDP dissociation inhibitor as a general regulator for the membrane association of Rab proteins. J Biol Chem 268, 18143–18150.

Ungermann C, Nichols BJ, Pelham HRB, Wickner W (1998). A vacuolar v-t-SNARE complex, the predominant form in vivo and on isolated vacuoles, is disassembled and activated for docking and fusion. J Cell Biol 140, 61–69.

van der Kant R, Fish A, Janssen L, Janssen H, Krom S, Ho N, Brummelkamp T, Carette J, Rocha N, Neefjes J (2013). Late endosomal transport and tethering are coupled processes controlled by RILP and the cholesterol sensor ORP1L. J Cell Sci 126, 3462–3474.

Vergne I, Chua J, Lee H-H, Lucas M, Belisle J, Deretic V (2005). Mechanism of phagolysosome biogenesis block by viable Mycobacterium tuberculosis. Proc Natl Acad Sci USA 102, 4033–4038.

Wang L, Merz AJ, Collins KM, Wickner W (2003). Hierarchy of protein assembly at the vertex ring domain for yeast vacuole docking and fusion. J Cell Biol 160, 365–374.

Weber T, Zemelman BV, McNew JA, Westermann B, Gmachl M, Parlati F, Söllner TH, Rothman JE (1998). SNAREpins: minimal machinery for membrane fusion. Cell 92, 759–772.

Wickner W, Rizo J (2017). A cascade of multiple proteins and lipids catalyzes membrane fusion. Mol Biol Cell 28, 707–711.

Zhao M, Wu S, Zhou Q, Vivona S, Cipriano DJ, Cheng Y, Brunger AT (2015). Mechanistic insights into the recycling machine of the SNARE complex. Nature 518, 61–67.

Zick M, Orr A, Schwartz ML, Merz AJ, Wicker WT (2015). Sec17 can trigger fusion of trans-SNARE paired membranes without Sec18. Proc Natl Acad Sci USA 112, E2290–E2297.